Identification of Long Non-Coding RNA Expression Profiles and Co-Expression Genes in Thyroid Carcinoma Based on The Cancer Genome Atlas (TCGA) Database

Authors' Contribution:
Study Design A
Data Collection B
Statistical Analysis C
Data Interpretation D
Manuscript Preparation E
Literature Search F
Funds Collection G

B Yun Zhang*
C Taobo Jin*
D Haipeng Shen
E Junfeng Yan
F Ming Guan
AG Xin Jin

Department of Endocrine Surgery, Zhuji People's Hospital of Zhejiang Province, Zhuji, Zhejiang, P.R. China

Corresponding Author:
Source of support:

* Yun Zhang and Taobo Jin contributed equally to this work
Xin Jin, e-mail: jinxinzhuji@outlook.com
Departmental sources

Background: Thyroid carcinoma is a malignancy with high morbidity and mortality. Genetic alterations play pivot roles in the pathogenesis of thyroid carcinoma, where long noncoding RNA (lncRNA) have been identified to be crucial. This study sought to investigate the biological functions of lncRNA expression profiles in thyroid carcinoma.

Material/Methods: The lncRNAs expression profiles were acquired from The Cancer Genome Atlas (TCGA) database according to 510 thyroid cancer tissues and 58 normal thyroid tissues. By using R package edgeR, differentially expressed RNAs were obtained. Also, an overall survival model was established based on Cox regression and clinical data then testified by Kaplan-Meier plot, receiver operating characteristic (ROC)-curve and C-index analysis. We investigated the co-expressed genes with lncRNAs involved in the prognostic model, as well as Gene Ontology (GO) and Kyoto Encyclopedia of Genes and Genomes (KEGG) pathway analysis was conducted R package clusterProfile.

Results: A total of 352 lncRNAs were identified as differentially expressed in thyroid carcinoma, and an overall survival model consisting of 8 signature lncRNAs was proposed (ROC=0.862, C-index=0.893, P<0.05), 3 of which (DOCK9-DT, FAM111A-DT, and LINC01736) represent co-expressed mRNAs. However, as an oncogene, only FAM111A-DT increased the prognostic risk in thyroid carcinoma. Furthermore, we found differential genes LINC01016, LHX1-DT, IGF2-AS, ND MIR1-1HG-AS1, significantly related to lymph node metastasis (P<0.05).

Conclusions: In this study, we clarified the differential lncRNA expression profiles which were related to the tumorigenesis and prognosis in thyroid carcinoma. Our results provide new rationale and understandings to the pathogenesis and regulatory mechanisms of thyroid carcinoma.

MeSH Keywords: Carcinogenesis • RNA, Long Noncoding • Thyroid Neoplasms

Full-text PDF: https://www.medscimonit.com/abstract/index/idArt/917845

📄 2162   ▦ 5   📊 7   📖 35

Background

Thyroid carcinoma is one of the most malignant tumors and it is postulated that morbidity and mortality by thyroid carcinoma in USA are increasing observed in 2019 [1]. Pathologically, papillary thyroid carcinoma (PTC) represents 80% of thyroid tumors which derived from parafollicular C-cells, where follicular-cell originated carcinomas are most common. Except for PTC, follicular thyroid carcinoma (FTC) (15%), poorly differentiated thyroid carcinoma (PDTC) (<2%) and anaplastic thyroid carcinoma (ATC) (<2%) have constituted follicular cell-derived thyroid carcinoma. FTC and PDTC have a decent prognosis, while ATC has high mortality a survival 3-month to 5-month survival rate after first diagnosis [2,3]. Over the past few decades, the increased incidence of thyroid carcinoma is not only attributed to environmental changes, but also mainly attributed to improvements in early diagnosis of thyroid carcinoma [4–6]. Although thyroid carcinoma is a multifactorial disease (as many studies have shown), pathogenesis, including genetic alternations, plays vital roles in carcinogenesis. The phosphatidylinositol-3-kinase PI3K/AKT and mitogen-activated protein kinase (MAPK) has been extensively revealed alternations in thyroid carcinoma with different molecular mechanisms [7–9].

With the development of high-throughput sequencing technologies, more than 20 000 lncRNAs have been drawn attentions since these noncoding transcripts were regarding as gene trash elements before [10]. It is widely recognized that lncRNAs are participated in the regulation of transcription, splicing, translation, and imprinting [11–15]. Increasing studies of lncRNAs show that they play vital roles in various human disease, especially in cancer [16,17], where lncRNAs may exhibit as tumorigenic or tumor suppresser genes. Ding et al. demonstrated that lncRNA *TPTEP1* could inhibit hepatocellular carcinoma cell development and occurrence by controlling IL-6/STAT3 signaling [18]. Yu et al. suggested *AFAP1-AS1* was an oncogenic gene and that the AFAP1-AS1/LSD1/HBP1 axis could be a new therapeutic target in non-small cell lung cancer [19]. Similarly, thousands of lncRNAs are involved in tumorigenesis in thyroid carcinoma, but the characterization of differential lncRNA expressions and functional profiles in thyroid carcinoma remain unclear.

In our study, we sought to analyze the differentiated lncRNA profiles in thyroid carcinomas by extracting from The Cancer Genome Atlas (TCGA) database. Additionally, investigated the relationship between differentiated lncRNAs and overall survival rate on patients. Also, Gene Ontology (GO) and Kyoto Encyclopedia of Genes and Genomes (KEGG) functional analyses were conducted to show the functional mRNAs. To this end, we demonstrated that the lymph node metastasis was associated lncRNAs. Taken together, our results provide new insights for tumorigenesis and lncRNA related pathogenesis in thyroid carcinoma.

Material and Methods

Datasets and differentially expressed lncRNAs

The transcriptome profiling data of 510 thyroid carcinoma samples and 58 normal thyroid samples were obtained from The Cancer Genome Atlas (TCGA) in January 2019. The lncRNA sequencing data and related clinical information were generated and we download them by utilizing The GDC Data Transfer Tool (*https://gdc.cancer.gov/access-data/gdc-data-transfer-tool*). Our study abides by the TCGA publication guidelines (*http://cancergenome.nih.gov/publications/publicationguide-lines*). By comparing thyroid carcinoma tissues to normal tissues and using R package edgeR in R software (version 3.4.1), differentially expressed lncRNAs were identified with thresholds |log2FoldChange| >2 as well as adjusted *P* value <0.05. The lncRNAs were annotated by ENSEMBL (*htps://www.ensembl.org/*) and depicted using the pheatmap package in R program. Ethical consent was not required because all the data in this study were obtained from the TCGA database.

Cox regression and survival analysis

All differentially expressed lncRNAs were subjected to univariate Cox regression with *P* value cutoff <0.01. Then the significant lncRNAs which related to univariate Cox regression were subsequently analyzed in a multivariate Cox proportional hazards model. By following the results of the multivariate Cox model and median risk score point, a total of 251 patients were grouped into "High risk" and "Low risk" respectively, where the risk score formula was shown as following:

Risk score=βgene 1× exprgene 1+ βgene 2× exprgene 2+: : + βgene n× exprgene n [20]. Cox regression analysis and Kaplan-Meier survival analysis were performed by using R package "survival". The receiver operating characteristic (ROC)-curve analysis and C-index analysis were conducted to evaluate the consequence of the risk system we established, which were performed by using R package survivalROC and BiocManager, respectively. The log-rank test was employed to evaluate the statistical differences in overall survival, and survival curves were depicted by Kaplan-Meier analysis, where *P*<0.05 was considered as statistically significant.

LncRNAs-proteins correlations

The correlations between differentially expressed lncRNAs and related mRNAs were determined by using package limma in R program. The minimum interaction absolute value was set at medium confidence 0.400 with *P* value cutoff <0.001. Based on the results, all correlated genes were submitted to functional enrichment analysis for further validation.

Functional analysis

In order to demonstrate the biological functions of the differential expressed lncRNAs which involved in our predictive model, functional enrichment analysis was performed by analysis of GO and KEGG pathway. By analyzing all the lncRNAs correlated genes, as indicated, we used clusterProfiler package in R software to determine the molecular function, biological process and cellular component for GO analysis and pathway analysis in KEGG. The histograms for GO and KEGG were acquired by the R package GOplot.

LncRNAs related to lymph nodes metastasis

A total of 352 differentially expressed lncRNAs, as indicated, were analyzed in relation to 230 nonlymph nodes metastasis (N0) patients and 225 lymph nodes metastasis (N1) with thresholds |log2FoldChange| >2 as well as adjusted *P* value <0.05. Moreover, these lncRNAs which link to lymph nodes metastasis were visualized using the pheatmap package in R program.

Results

Differentially expressed lncRNAs in thyroid carcinoma

A total of 352 lncRNAs were identified as differentially expressed in thyroid carcinoma (510 thyroid carcinoma samples versus 58 normal thyroid tissues) (Supplementary Table 1). Of these, 166 lncRNAs (47.2%) were considered to be downregulated while 186 lncRNAs (52.8%) were upregulated. By visualizing the lncRNAs expression profiles, we performed volcano plot and heatmap to depict the overall differences among each gene (Figure 1A, 1B).

Cox regression and overall survival model

A total of 352 differentially expressed lncRNAs were determined with univariate Cox analysis, as shown in Table 1. We found 12 lncRNAs to be significantly related to overall survival with univariate Cox regression at a significant level of *P*<0.01. Subsequently, we then performed a multivariate Cox regression analysis where a total 8 lncRNAs were found to be as coupled to a prognosis model for overall survival (P=5.2405e-06), of which *DOCK9-DT, LINC00900, C8orf34-AS1, LINC01736* were suggested as protective factors while *ATP2C2-AS1, FAM111A-DT, LINC02550, LINC01896* increased the risk in thyroid carcinoma (Figure 2). However, *ATP2C2-AS1* and *LINC02550* were downregulated genes, where the other 6 genes determine the opposite functions (Table 2). According to the overall survival model, we grouped patients into "high risk" and "low risk" groups, where the high-risk patients showed worse overall survival to low-risk group (*P*=1.0627e-04) (Figure 3A).

Additionally, ROC-curve analysis depicted the discriminative value of our established risk scoring system, where we found an AUC=0.862 (Figure 3B). Our risk scoring system was found to be highly sensitivity and specificity (100% and 94%) respectively in predicting overall survival, and the high-risk scoring group could be used for an impressive method for overall survival prediction. The heatmap represents the expression profiles of overall survival model based on the risk scoring system (Figure 3C). Also, we calculated the C-index value of our overall survival model, which is well proven (Table 3). Furthermore, the risk scores and survival status of all patients were visualized in Figure 4A and 4B where high-risk patients were significantly correlated to death as expected. Only 1 patient dead in the low-risk group (0.4%), while 15 patients dead in high-risk group (6.0%). Together, these data demonstrated that the impressive overall survival model based on the Cox regression could be a decent method for prognosis prediction.

LncRNAs correlated mRNAs and functional analysis

A total of 3 lncRNAs (*DOCK9-DT, FAM111A-DT,* and *LINC01736*) were involved in the overall survival model and were found to be correlated to mRNAs expressions which co-expressed with 3274, 3412, and 31 mRNAs respectively. Based on the predicted Pearson correlation score, the top 5 correlating mRNAs of *DOCK9-DT, FAM111A-DT,* and *LINC01736* are presented in Figure 5. We found a significantly strong correlation between *DOCK9-DT* and *SDC4* (Cor=0.826, *P*=6.156e-143) and between *FAM111A* and *FAM111A-DT* (Cor=0.839, *P*=2.212e-151).

To further investigate the biological functions of these co-expressed mRNAs, we conducted GO and KEGG functional analysis. As shown in Figure 6A, the results indicated that for GO analysis, most of the mRNAs were assembled in cell adhesion molecule binding with the lowest *P*-value at 8.33e-05 in *FAM111A-DT* while oxidoreductase activity, acting on the aldehyde or oxo group of donors represented the lowest *P*-value 6.82e-05 in *DOCK9-DT*. In addition, a total of 4 mRNAs were related to phospholipid binding in *LINC01736*. By analyzing the results of KEGG enrichment pathways, we found that in *DOCK9-DT*, a total of 70 genes were gathering in MAPK signaling pathway, while human papillomavirus infection reflects the most significant pathway including 85 genes in *FAM111A-DT* and *Staphylococcus aureus* infection represents the highest cancer associated pathway in *LINC01736* (Figure 6B). These results indicated that these 3 lncRNAs might play vital roles in the tumorigenesis by targeting functional mRNAs.

Lymph nodes metastasis-related lncRNAs

Since lymph nodes metastasis is a critical predictive factor in thyroid carcinoma [21,22], we further analyzed the relationship between differentially expressed lncRNAs and lymph nodes
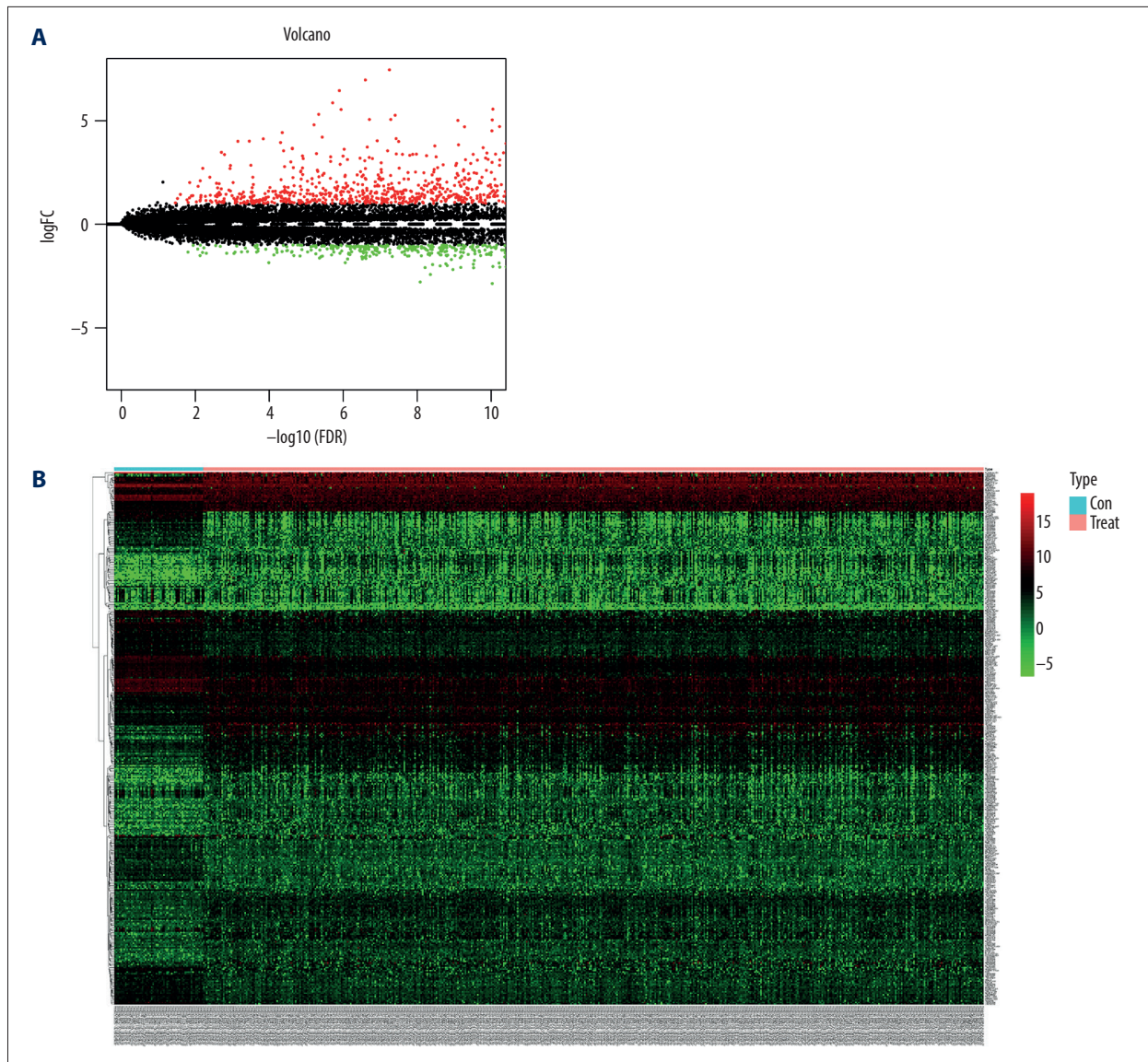
Figure 1. Differentially expressed lncRNAs in thyroid carcinoma. (**A**) Volcano plots show the distribution of differentially expressed lncRNAs. Upregulated lncRNAs were represented by red dots while the downregulated lncRNAs were represented by green dots. (**B**) Heatmap volcano plots show the distribution of differentially expressed lncRNAs, Red color represent up-regulated lncRNAs while the green color represents downregulated lncRNAs. lncRNAs – long noncoding RNAs.

metastasis. Among 352 differentially expressed lncRNAs, we found that 4 upregulated genes (*LINC01016, LHX1-DT, IGF2-AS*, and *MIR1-1HG-AS1*) were significantly expressed across patients with N1 than N0 (Table 4), and the results were visualized by heatmap (Figure 7).

Discussion

The screening of RNAs transcripts was facilitated in the past 20 years and lncRNAs were testified to be an emerging factor which strongly associated with tumorigenesis and metastasis

in thyroid carcinoma [23–26]. To understand the mechanism of genetic and epigenetic alterations in thyroid carcinoma, we investigated the transcriptomes files of thyroid carcinoma and normal thyroid samples based on TCGA database. We clarified that some lncRNAs have significantly interactions with overall survival, and the predictive survival model was established where some gene expression signatures were well elucidated. Furthermore, *LINC01016, LHX1-DT, IGF2-AS,* and *MIR1-1HG-AS1* showed the possibility related to lymph node metastasis in the thyroid.

Table 1. Significant lncRNAs in univariate Cox regression ($P<0.01$).

Gene	HR	z	P-value
LINC00900	0.578188577	−3.232009209	0.001229231
LINC02471	0.799698308	−3.18117259	0.001466802
LINC02550	1.587458096	3.109803736	0.001872117
DOCK9-DT	0.507389188	−3.021875971	0.002512135
LINC02555	0.814930817	−2.888049273	0.003876391
ATP2C2-AS1	1.929219328	2.841530213	0.00448976
LINC01896	1.317107839	2.767740738	0.005644634
FAM111A-DT	0.510951459	−2.708395538	0.006760939
PAX8-AS1	2.027929479	2.620760006	0.0087734
C8orf34-AS1	0.660496757	−2.601271103	0.009287902
LINC01929	1.549979462	2.599584878	0.009333659
LINC01736	0.631751329	−2.580697317	0.009860099
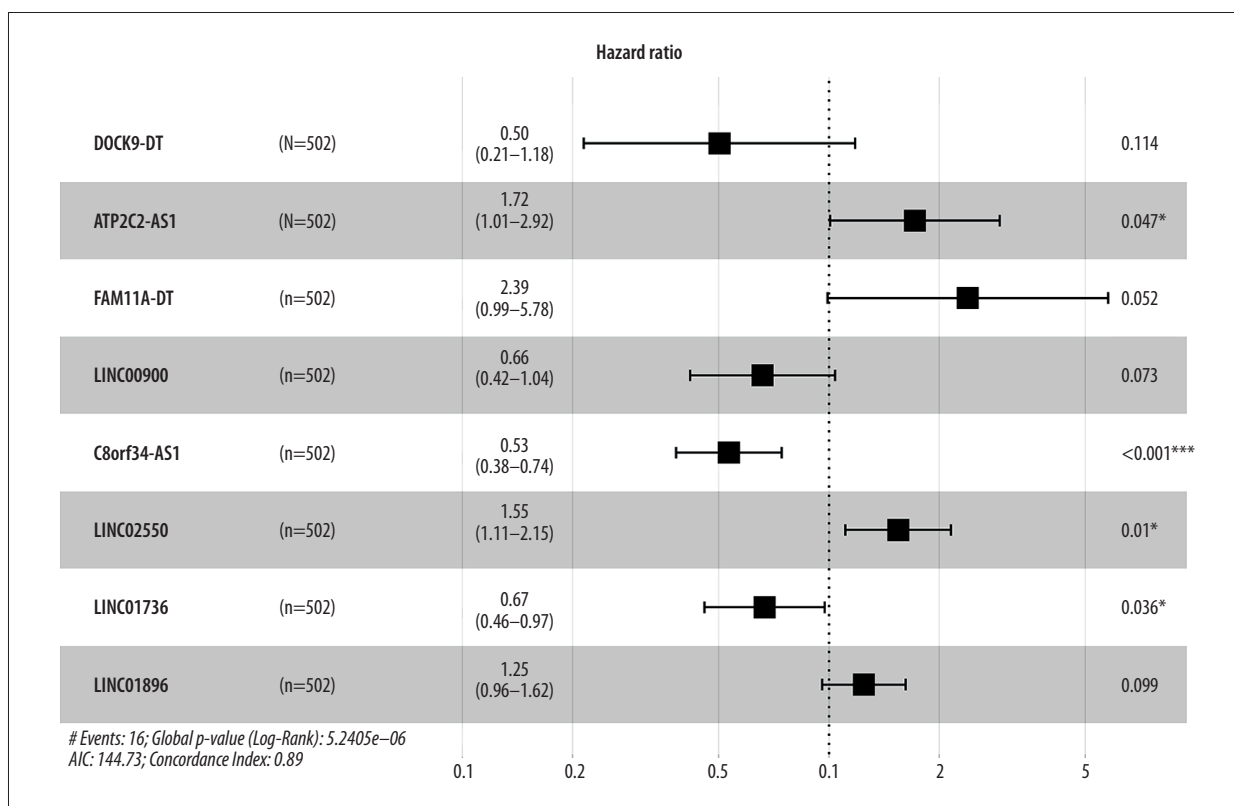
Figure 2. Eight lncRNA expression profiles for prediction of overall survival in thyroid carcinoma by multivariate Cox regression. lncRNA – long noncoding RNA.

We found in our overall survival prediction survival model that *DOCK9-DT, LINC00900, C8of34-AS1,* and *LINC01736* exerted as protective factors in prognosis, while *ATP2C2-AS1, FAM111A-DT, LINC02550,* and *LINC01896* increased the risks; however, only *FAM111A-DT* and *LINC02550* exerted as oncogenes in thyroid carcinoma as well as significantly positively correlated with poor outcomes in patients. Interestingly, these lncRNAs have not been reported or studied before, the prognostic value of these bundles of genes and our overall survival model remains to be confirmed and demonstrated.

Table 2. Differentially expressed lncRNAs in overall survival model.

DElncRNAs	Regulation	Log fold change	FDR
DOCK9-DT	Upregulation	1.907135801	3.87E-38
LINC00900	Upregulation	1.122886421	5.38E-18
C8orf34-AS1	Upregulation	1.431387442	4.08E-08
LINC01736	Upregulation	1.001949864	0.000258681
ATP2C2-AS1	Downregulation	−1.382854376	4.18E-24
FAM111A-DT	Upregulation	1.317334235	5.38E-24
LINC02550	Downregulation	−1.012245336	1.46E-05
LINC01896	Upregulation	2.692433265	0.006280554
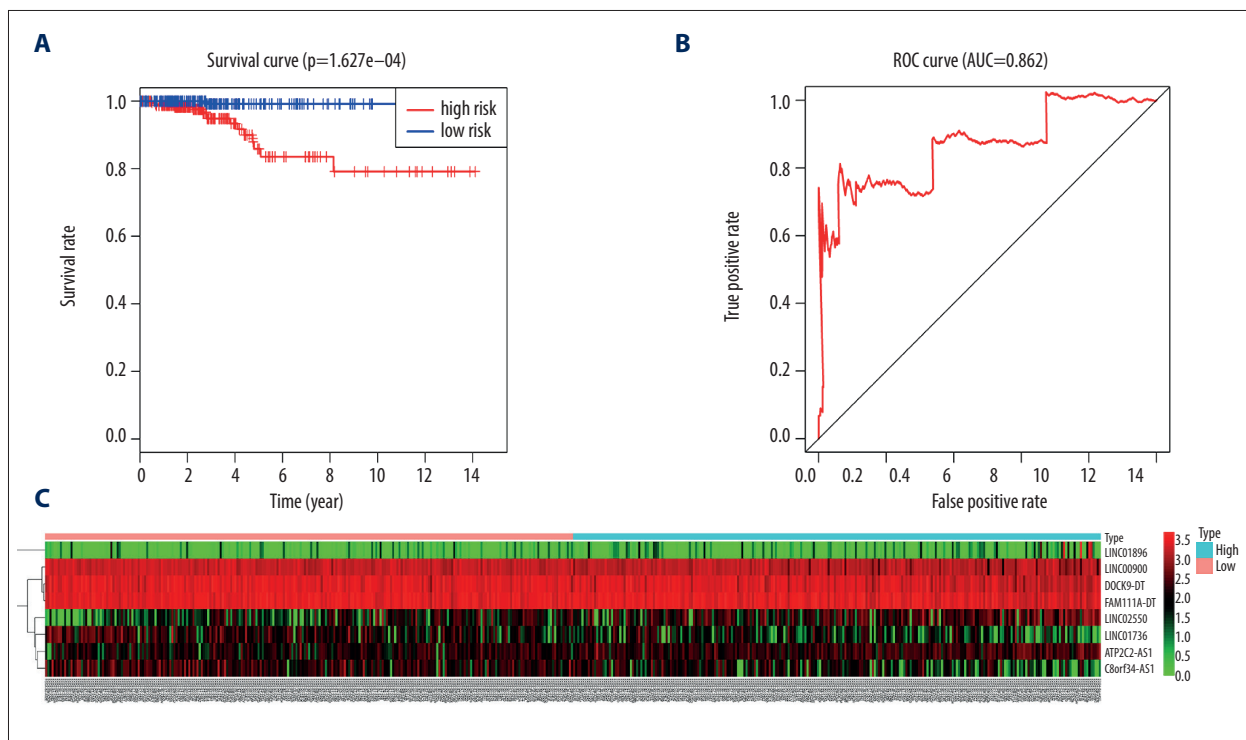
Figure 3. Cox regression and overall survival model. (**A**) Kaplan Meier plot showed significance between high-risk and low-risk patients in overall survival by the prognostic model (*P*<0.05). (**B**) The ROC curve analysis for the overall survival model (AUC=0.862) (**C**) The heatmap of 8 lncRNA expression profiles for prediction of overall survival model. ROC – receiver operating characteristics; AUC – area under the ROC; lnRNA – long noncoding RNA.

Table 3. C-index value of the overall survival model.

C-index	SE	Lower	Upper	P-value
0.8926066	0.04260484	0.8091026	0.9761105	3.110781e-20

Previous results [27] suggested that *FAM111A-DT* could be the most promising genes in tumorigenesis of thyroid carcinoma, by numerous binding mRNAs with high correlation index. *FAM111A-DT*, which named as FAM111A divergent transcript, ubiquitously expressed in 25 tissues including thyroid gland.

This study validated that there is a significant correlation between *FAM111A-DT* and *FAM111A*, which confirmed early findings [28] that new susceptibility *loci* reached on chromosomes 11q12 (FAM111A-FAM111B) were linked to the carcinogenesis of prostate cancer. Fernandez et al. indicated that *FAM111A*

Figure 4. (**A**) Scatter diagram showed risk scores of thyroid carcinoma patients based on TCGA database. (**B**) Scatter diagram showed survivals statues of thyroid carcinoma patients based on TCGA database. TCGA – The Cancer Genome Atlas.
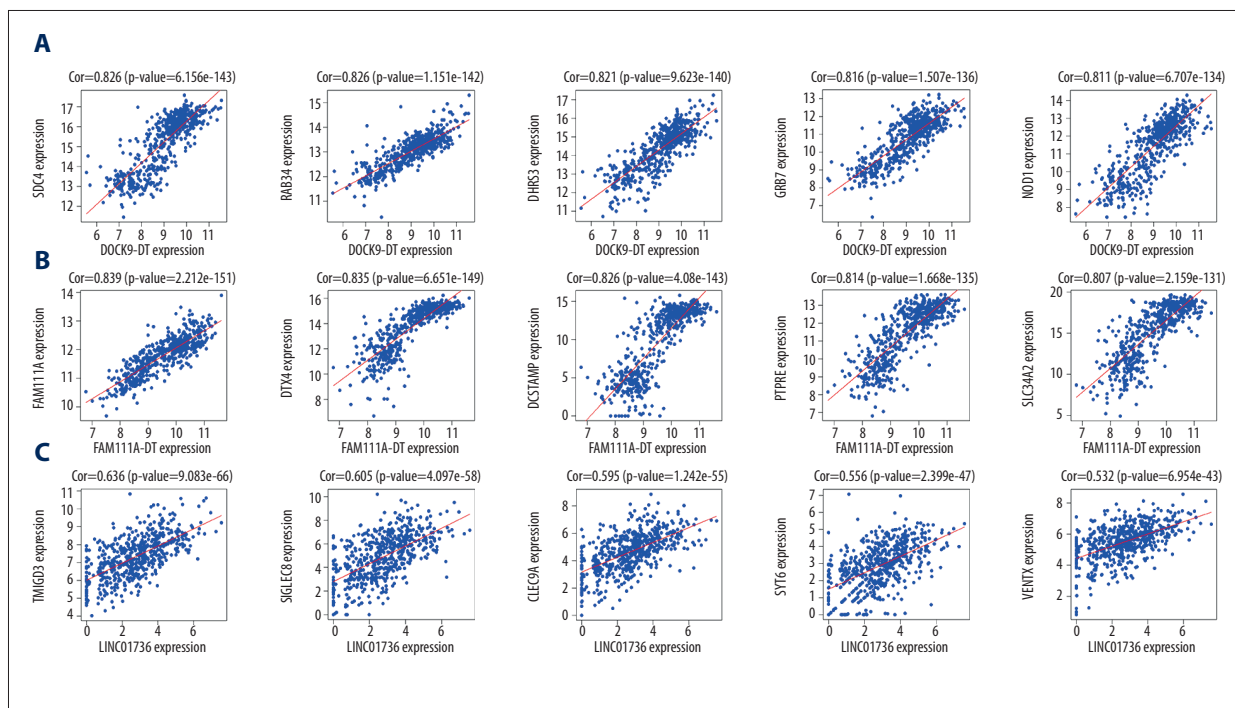
Figure 5. The correlation plots between differentially expressed lncRNAs and mRNAs. (**A**) The correlation plots of the top 5 correlated mRNAs of *DOCK-DT*. (**B**) The correlation plots of the top 5 correlated mRNAs of 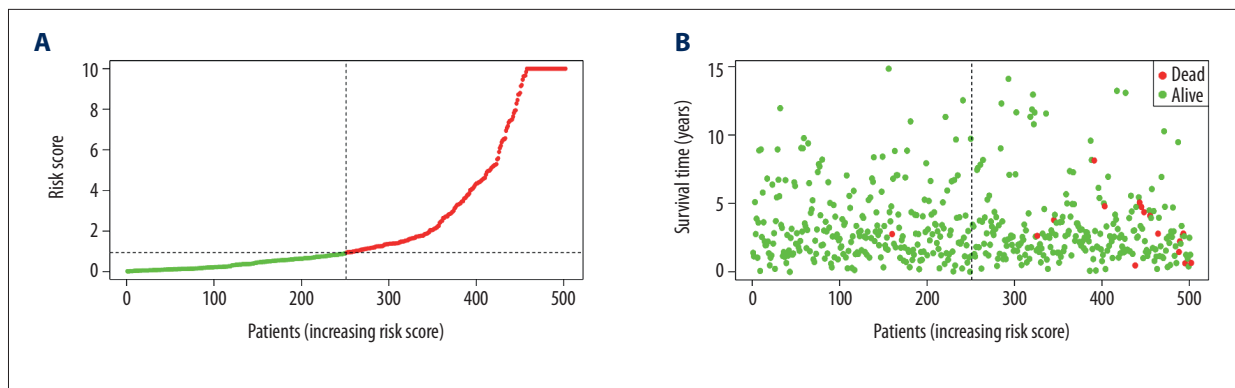*FAM111A-DT*. (**C**) The correlation plots of the top 5 correlated mRNAs of *LINC01736*. lncRNAs – long noncoding RNAs, mRNA – messenger RNA.

expression could predict the possibility of local advanced cervical cancer patients who are developing distal metastasis [29]. Our results showed for thyroid carcinoma were consistent with these previous studies, suggesting the relations of *FAM111A* with tumorigenesis and prognosis. Additionally, 3 (*DCSTAMP*, *PTPRE,* and *SLC34A2*) of top 5 correlated genes of *FAM111A-DT* were reported to be positively correlated with the development of thyroid carcinoma [30-33]. However, biologically, functional experiments and larger cohort studies should be performed in the future to further explain the molecular mechanisms of *FAM111A-DT* in thyroid carcinoma as it only showed a trend in the Cox proportional hazards model (*P*=0.052)

It is well known that the clinicopathological features, such as distal tumor metastasis and lymph node metastasis, as well tumor grade or staging have been proven to be pivotal prognostic factors in thyroid carcinoma, but the relationship with lncRNAs expression profiles remains obscured. In our study, one of the novel and potentially important findings was that *LINC01016, LHX1-DT, IGF2-AS,* and *MIR1-1HG-AS1* were significantly linked to tumorigenesis and lymph node metastasis. None of the lncRNAs have been investigated except *IGF2-AS*. It has been proposed that *IGF2* encodes a member of the insulin family of polypeptide growth factors, which promote growth-promoting activity possess. Consequently, as
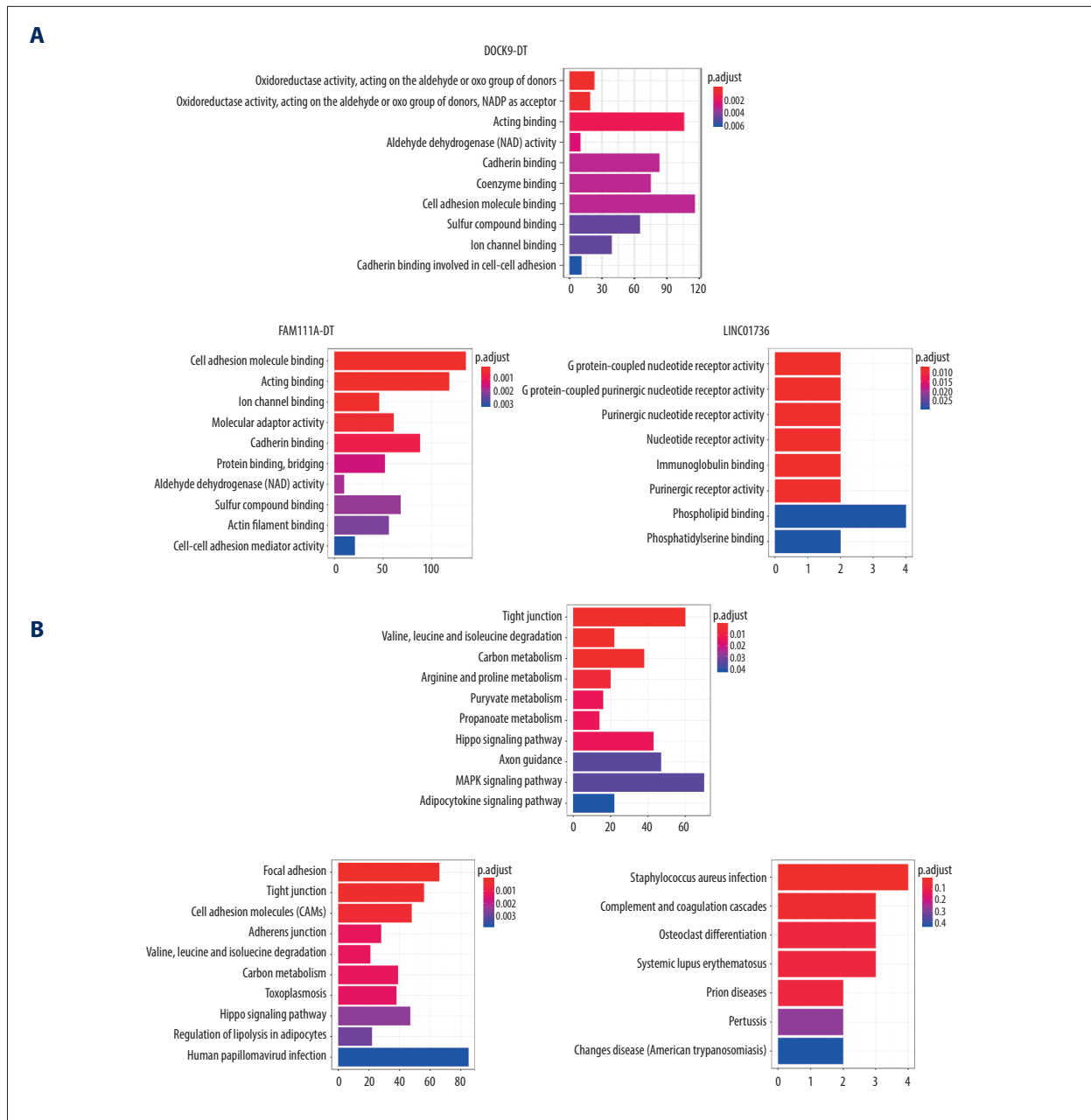
Figure 6. Functional enrichment analysis for *DOCK-DT*, *FAM111A-DT*, and *LINC01736* co-expressed genes. (**A**) Top 10 biological processes of GO analysis. (**B**) Top 10 pathways of KEGG enrichment analysis. GO – Gene Ontology; KEGG – Kyoto Encyclopedia of Genes and Genomes.

Table 4. Differentially expressed LncRNAs related to lymph node metastasis.

DElncRNAs	Regulation	Log fold change	FDR
LINC01016	Upregulation	3.865146393	1.06E-28
LHX1-DT	Upregulation	5.243275683	6.43E-28
IGF2-AS	Upregulation	5.085826129	8.86E-38
MIR1-1HG-AS1	Upregulation	4.019136688	8.86E-38
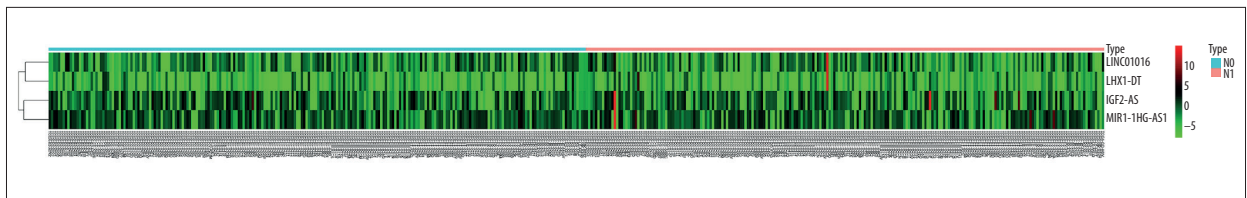
Figure 7. A heatmap of differentially expressed lncRNAs associated with lymph node metastasis. lncRNAs – long noncoding RNAs.

an antisense RNA of *IGF2*, *IGF2-AS* plays an important role in various cancers, including neuroblastoma and prostate cancer [34,35]. However, the function of *IGF2-AS* in thyroid carcinoma has not been elucidated yet; larger cohort is needed to testify the role and mechanisms.

Conclusions

We have identified differentially expressed lncRNAs based on TCGA database which associated with oncogenesis and prognosis of thyroid carcinoma. Although many lncRNAs showed promising and novel roles as biomarkers, lack of literature support limits the determinacy of these gene signatures. Future mechanistic studies are needed to validate these finding using functional experiments *in vivo* and *in vitro*. Importantly, our study provides new understandings for future studies of lncRNAs in thyroid carcinoma.

Conflicts of interests

None.

Supplementary Data

Supplementary Table 1. A list of 352 differentially expressed lncRNAs.

| LncRNA	logFC	logCPM	PValue	FDR
ADD3-AS1	−1.544462734	−0.99910347	7.41E-64	2.41E-61
LINC01977	3.843510161	0.480401174	3.30E-62	9.70E-60
RUNDC3A-AS1	1.952999031	2.819115059	1.60E-57	3.27E-55
LINC02454	4.588997022	0.89782849	1.61E-57	3.27E-55
LINC02580	−2.495858713	−2.236797796	5.59E-57	1.09E-54
STK32A-AS1	3.034463136	1.065838602	1.13E-54	1.85E-52
ST7-AS1	−1.448121092	1.639916538	3.98E-53	5.75E-51
LINC02471	5.322739754	3.409062735	4.33E-53	6.20E-51
GASAL1	−1.59528068	−1.059362756	5.43E-51	6.43E-49
UNC5B-AS1	4.973040329	0.130580513	5.60E-51	6.59E-49
ATP2B1-AS1	−1.307528781	1.422251738	3.19E-50	3.59E-48
LPP-AS2	−1.308820155	0.367428007	4.66E-50	5.12E-48
LNCTAM34A	1.644647087	0.883915622	1.87E-48	1.74E-46
LINC02432	−2.182366897	0.003975372	2.50E-48	2.30E-46
SEPT7-AS1	−1.271664294	1.166809574	5.28E-47	4.43E-45
LINC01354	−2.298558579	−0.743544878	5.17E-46	3.95E-44
LRP4-AS1	4.203658018	−0.081468552	5.23E-44	3.24E-42
STARD13-AS	−1.594861034	−1.853468472	9.54E-44	5.81E-42
LINC02158	−1.762893598	−2.434775175	6.45E-43	3.65E-41
LINC02560	3.846613199	1.279411649	4.80E-41	2.34E-39
LYPLAL1-DT	−1.420355734	−2.28151519	1.36E-40	6.33E-39
HAGLROS	3.855538988	−0.487304666	1.88E-40	8.69E-39
LINC02555	6.186581911	4.08600787	8.26E-40	3.63E-38

LncRNA	logFC	logCPM	PValue	FDR
DOCK9-DT	1.907135801	3.415634107	8.85E-40	3.87E-38
TNRC6C-AS1	2.5220245	4.460828007	7.03E-39	2.85E-37
LINC01770	3.033484056	0.776786468	9.92E-39	3.95E-37
LINC01539	−2.546623831	−0.740040233	2.60E-38	1.01E-36
LINC01672	−2.533325932	−2.658901068	4.37E-38	1.66E-36
LINC01220	−1.429512524	−1.210742776	9.94E-38	3.65E-36
TDRKH-AS1	1.38188595	0.208416671	1.17E-37	4.24E-36
LINC02408	5.147620444	1.193102388	4.21E-37	1.47E-35
LINC02082	4.770468911	−0.653572663	6.00E-37	2.06E-35
RARA-AS1	1.443101238	2.55332964	1.83E-36	6.13E-35
NR2F1-AS1	2.897311389	3.854469179	4.54E-36	1.48E-34
OR2A1-AS1	−1.209175922	2.558663714	8.10E-36	2.59E-34
LINC01135	−1.3665171	0.464057321	5.03E-35	1.52E-33
LINC00514	2.298637682	−0.957251179	7.57E-35	2.26E-33
LINC01725	−1.164413145	−0.30010055	1.32E-34	3.86E-33
LINC01170	3.882335006	−1.25756306	1.35E-34	3.95E-33
MIR181A2HG	1.95070326	2.023625063	6.77E-34	1.87E-32
MIR34AHG	1.622572953	−2.521191582	1.46E-33	3.94E-32
SMAD9-IT1	−1.920493079	−2.093723565	1.58E-33	4.27E-32
LINC01460	3.604749946	−1.925216927	1.98E-33	5.28E-32
ARHGAP31-AS1	−1.11772071	−1.21269273	2.12E-33	5.63E-32
LIFR-AS1	−1.457762348	2.018345953	3.78E-33	9.79E-32
LANCL1-AS1	−1.258442476	−2.003689732	5.84E-33	1.49E-31
MIR22HG	−1.304486022	4.882887133	8.82E-33	2.23E-31
SNHG26	−1.299920087	−1.076357115	3.09E-32	7.51E-31
CASC2	−1.005091664	2.59711651	4.02E-32	9.64E-31
KCNJ2-AS1	1.8599128	2.203800758	4.31E-32	1.03E-30
LNCNEF	−3.203013222	−1.298660925	6.62E-32	1.55E-30
LINC02028	−1.680320937	0.244417604	2.17E-31	4.87E-30
TPRG1-AS1	−1.918207633	−2.448867715	2.38E-31	5.33E-30
MORC2-AS1	−1.32573386	−2.189107706	4.21E-31	9.19E-30
CYP1B1-AS1	2.047482448	0.864661895	5.08E-31	1.10E-29
PAX8-AS1	−1.219726528	3.101518779	1.62E-30	3.37E-29
LINC01140	−1.425900765	−0.632067519	8.84E-30	1.74E-28
FOXD2-AS1	1.578373644	0.546358741	1.59E-29	3.09E-28
TBC1D8-AS1	−1.36022454	0.389079523	2.50E-29	4.75E-28
LINC00511	3.120031564	1.742540436	7.18E-29	1.32E-27
LINC01361	−1.760659712	−3.12804555	8.96E-29	1.63E-27
PCAT14	−2.687359418	−1.036548014	1.20E-28	2.15E-27
WWC2-AS2	−1.004596422	−0.001346254	2.02E-28	3.60E-27
ATP6V0E2-AS1	−1.668598995	2.020920917	2.17E-28	3.85E-27
LINC00472	−1.115635959	1.391387302	3.07E-28	5.35E-27
LINC00284	3.786361822	−0.425537055	5.14E-28	8.84E-27
CYP4A22-AS1	2.079699245	−2.603839908	6.87E-28	1.17E-26

LncRNA	logFC	logCPM	PValue	FDR
LBX2-AS1	1.463264557	1.755683621	8.58E-28	1.45E-26
RPL34-AS1	−1.203128176	−1.458432773	8.79E-28	1.48E-26
LINC01510	4.229541483	−1.319784443	3.05E-27	4.87E-26
SYNE1-AS1	−1.966150668	−2.977194055	3.09E-27	4.93E-26
BLACAT1	1.279741871	3.02231177	3.10E-27	4.93E-26
KCNMB2-AS1	3.030847157	−2.797887475	3.19E-27	5.06E-26
FAM170B-AS1	4.141213927	−2.095343957	5.85E-27	9.08E-26
LINC01747	3.363198671	−1.267611404	6.05E-27	9.36E-26
MPPED2-AS1	−2.779933864	−0.982180517	6.64E-27	1.02E-25
SNRK-AS1	−1.562113657	−1.628548226	1.10E-26	1.67E-25
DCST1-AS1	1.126217274	0.287018235	1.13E-26	1.72E-25
A2M-AS1	−1.079797666	0.138315547	1.55E-26	2.33E-25
LINC01137	1.085515411	2.72440927	2.30E-26	3.38E-25
LINC00891	2.471054911	−0.421841494	2.34E-26	3.45E-25
LINC01483	2.591772438	−0.607502062	5.15E-26	7.36E-25
ATP2C2-AS1	−1.382854376	−1.749749778	3.12E-25	4.18E-24
LINC00607	2.563986409	0.766391856	3.68E-25	4.88E-24
FAM111A-DT	1.317334235	3.855342682	4.07E-25	5.38E-24
KIZ-AS1	−1.361427086	−2.770024349	5.53E-25	7.25E-24
HAGLR	3.234842305	2.671591247	9.06E-25	1.17E-23
LINC00092	−1.618940495	1.734189502	9.80E-25	1.26E-23
TMEM92-AS1	3.368339962	−2.700681873	1.56E-24	1.96E-23
LINC01136	−1.632608982	−3.043954188	1.77E-24	2.20E-23
LINC01126	−1.382875629	−1.345887254	2.16E-24	2.68E-23
LINC00926	−1.817451324	0.848548942	2.66E-24	3.27E-23
LINC02345	2.808452122	−0.709869138	3.40E-24	4.14E-23
SNX29P2	−1.774050433	−3.061371492	3.54E-24	4.31E-23
THRB-AS1	−1.228115348	−1.417597346	3.61E-24	4.38E-23
WDR11-AS1	−1.258406396	−1.879618996	4.62E-24	5.55E-23
LINC02308	−2.449471097	−2.99105361	6.72E-24	7.98E-23
LINC01918	2.321282876	−1.16545749	1.16E-23	1.35E-22
LINC00612	−1.559936503	−2.038929246	1.91E-23	2.18E-22
FAM230B	3.782245505	−2.337329278	2.66E-23	3.00E-22
CDKN2B-AS1	2.328544511	−1.37043268	4.54E-23	5.03E-22
DCTN1-AS1	2.320679064	−1.88162992	5.69E-23	6.27E-22
NAMA	−1.695862202	−2.785554453	9.82E-23	1.06E-21
MIR31HG	2.772960652	1.188940105	1.63E-22	1.72E-21
LINC01614	3.956293322	−1.066952898	1.65E-22	1.74E-21
ELN-AS1	−1.073619711	0.517815127	1.99E-22	2.07E-21
CLIP1-AS1	−1.396886915	−3.097080989	2.02E-22	2.10E-21
LINC01659	−2.151654666	−3.196071291	2.73E-22	2.82E-21
LINC02343	3.189374218	−2.726018715	3.24E-22	3.32E-21
LINC01267	2.401810281	−2.708906593	7.65E-22	7.67E-21
LINC00609	−1.636688954	−2.515383665	7.98E-22	7.98E-21

LncRNA	logFC	logCPM	PValue	FDR
DUXAP8	2.525692559	−1.151147476	9.78E-22	9.72E-21
IGFL2-AS1	3.834169818	−2.485637868	1.28E-21	1.26E-20
LINC00506	−1.384523233	−1.817503745	1.55E-21	1.52E-20
EIPR1-IT1	−1.434838641	−0.630233231	1.57E-21	1.54E-20
FLJ16779	3.911130592	1.140616515	3.60E-21	3.39E-20
LINC02532	−1.534790709	−1.322011292	3.77E-21	3.55E-20
LINC01508	−1.300535781	0.973363364	4.80E-21	4.49E-20
LINC01058	−1.203926684	−3.19792648	5.62E-21	5.22E-20
PLA2G4E-AS1	−1.206501944	−2.660510878	6.48E-21	5.99E-20
TCERG1L-AS1	2.049627044	−1.24742241	6.53E-21	6.03E-20
PARAL1	4.346540422	−1.773215312	1.68E-20	1.50E-19
FZD10-DT	−1.224093818	0.581477012	1.85E-20	1.65E-19
UCKL1-AS1	−1.165628262	−1.427590888	2.71E-20	2.39E-19
LINC00853	1.181203734	0.716576648	2.75E-20	2.42E-19
ADAMTSL4-AS1	−1.145373158	−1.336200098	2.85E-20	2.51E-19
GAPLINC	1.597181425	−1.712729512	2.99E-20	2.63E-19
LINC01975	−2.599270665	−2.300678546	3.88E-20	3.37E-19
TBILA	−1.261048077	1.918044245	1.05E-19	8.82E-19
LINC01550	−1.249560267	0.839350621	1.69E-19	1.39E-18
WWTR1-AS1	−1.017125584	0.223947847	2.38E-19	1.94E-18
LINC00887	2.432295808	1.135730954	2.46E-19	2.01E-18
LINC01426	1.898942986	−0.028798475	2.54E-19	2.06E-18
MID1IP1-AS1	−1.121699853	−1.710609277	4.35E-19	3.47E-18
LINC01985	−1.442639538	−3.009102531	5.77E-19	4.54E-18
TNFRSF10A-AS1	1.068417568	0.129805675	5.85E-19	4.61E-18
LINC01814	−1.067329139	−0.18296878	6.03E-19	4.74E-18
NCAM1-AS1	−1.876475157	−3.020185119	6.43E-19	5.04E-18
LINC00900	1.122886421	2.205956467	6.88E-19	5.38E-18
PGM5-AS1	−1.75993484	−2.956330535	7.04E-19	5.49E-18
LINC01836	−1.45054792	−0.716553598	8.73E-19	6.74E-18
HAND2-AS1	−1.800404947	−1.05377541	1.49E-18	1.13E-17
FAM181A-AS1	−1.666658115	−1.383650436	1.59E-18	1.20E-17
LINC02593	2.178998373	2.700036405	1.76E-18	1.33E-17
LEMD1-AS1	1.531899488	−1.539817408	1.95E-18	1.46E-17
LINC00167	−1.278875217	−2.971124274	2.30E-18	1.71E-17
LINC00460	3.331082757	−2.69009325	2.71E-18	2.00E-17
LINC01704	1.683732006	−2.733975495	4.26E-18	3.10E-17
SH3PXD2A-AS1	1.6288274	−2.35625687	4.36E-18	3.17E-17
LINC00982	−1.339058009	3.307059677	4.49E-18	3.26E-17
ZNF571-AS1	1.471778093	1.485743805	5.63E-18	4.06E-17
CATIP-AS2	−1.455702841	−2.102456882	7.83E-18	5.57E-17
HCG2040054	−1.071754441	−3.058694113	8.48E-18	6.01E-17
NADK2-AS1	−1.267928642	−2.345077894	1.05E-17	7.37E-17
FAM182A	−1.525124056	−2.387619015	1.65E-17	1.14E-16

LncRNA	logFC	logCPM	PValue	FDR
HCG22	2.53270204	2.327072427	1.82E-17	1.25E-16
LINC01237	−1.00802835	−0.903572011	2.40E-17	1.64E-16
VAC14-AS1	2.016076996	−1.403521888	4.29E-17	2.87E-16
SOX9-AS1	−1.377769233	0.522130732	5.26E-17	3.49E-16
TMEM108-AS1	4.047490713	−1.925055227	6.17E-17	4.07E-16
LINC02461	5.681571486	−1.639717846	8.87E-17	5.80E-16
LINC02257	3.694696068	−2.840992741	9.62E-17	6.27E-16
SFTA1P	2.027026167	−0.249630586	1.05E-16	6.83E-16
LINC01615	1.805083366	−1.800514029	1.22E-16	7.86E-16
LINC00942	1.832226061	−1.347501378	2.06E-16	1.30E-15
SEPT4-AS1	−1.108555124	−2.120539973	2.06E-16	1.30E-15
LINC01878	2.73742996	−1.282814414	3.20E-16	1.98E-15
NAV2-AS4	−1.646324166	−2.958418321	4.34E-16	2.65E-15
LINC02397	−2.191000823	−2.04893046	4.52E-16	2.76E-15
LINC02458	2.316587621	−2.438485876	4.68E-16	2.85E-15
NPSR1-AS1	4.778075117	−2.534793294	5.71E-16	3.45E-15
PTCSC3	−1.177246001	4.550725941	7.77E-16	4.62E-15
MYCNOS	−1.407429743	−2.457946908	7.82E-16	4.65E-15
LINC02603	1.328056569	−1.69712963	8.05E-16	4.78E-15
VWA8-AS1	−1.015148852	−2.94836486	9.69E-16	5.72E-15
MAL2-AS1	−1.150928064	−2.243454717	9.82E-16	5.79E-15
LINC00652	−1.277394523	−1.43802152	1.06E-15	6.24E-15
LINC00973	3.102991921	−1.550754305	2.22E-15	1.27E-14
LINC01176	1.20163737	0.820750186	2.27E-15	1.29E-14
LINC01204	3.258598913	−1.983867759	2.44E-15	1.39E-14
CD44-AS1	1.515316083	−0.730955415	3.10E-15	1.75E-14
LINC02427	−1.204613362	−1.982451891	3.47E-15	1.94E-14
EPHA5-AS1	−2.559138368	−2.263641061	3.73E-15	2.08E-14
LINC02407	2.775865459	−2.396862015	4.19E-15	2.33E-14
FAM167A-AS1	−2.200036412	−1.52167867	6.90E-15	3.77E-14
BANCR	−1.332417606	−1.864760416	6.99E-15	3.82E-14
PURPL	3.333287808	−1.858357554	7.51E-15	4.09E-14
ITPR1-DT	−1.400224026	−0.692911657	7.90E-15	4.29E-14
ZNF30-AS1	−1.050761875	−2.480148516	8.92E-15	4.82E-14
ACBD3-AS1	1.158294887	−1.414775844	9.43E-15	5.08E-14
ADGRD1-AS1	−1.504919287	−0.336427391	1.17E-14	6.25E-14
LINC00487	−1.600011056	−2.775968336	1.24E-14	6.63E-14
LINC01224	1.431342497	−1.163210302	1.34E-14	7.12E-14
LINC01711	2.790153991	−2.263546533	1.42E-14	7.52E-14
TM4SF1-AS1	2.700697832	−0.683459875	1.94E-14	1.02E-13
CASC15	1.394024769	0.905677061	2.32E-14	1.21E-13
GUSBP11	1.012835514	1.127426539	2.68E-14	1.39E-13
LINC02535	1.798338705	−2.385033926	3.04E-14	1.57E-13
LINC01303	−1.140793874	−2.399111555	4.08E-14	2.08E-13

LncRNA	logFC	logCPM	PValue	FDR
SNAP25-AS1	1.569949042	−1.979043961	4.81E-14	2.44E-13
HRAT5	−1.019022797	−2.156656649	6.66E-14	3.34E-13
LINC01571	−1.199548925	2.322342254	7.30E-14	3.65E-13
LINC02600	2.337990299	0.442796118	8.40E-14	4.18E-13
DGUOK-AS1	1.040714475	0.964024802	8.57E-14	4.25E-13
UBXN10-AS1	1.017097011	1.005779667	9.08E-14	4.50E-13
SPANXA2-OT1	1.300402877	−2.217204778	1.28E-13	6.28E-13
FMR1-AS1	−1.067781104	−2.963904243	1.42E-13	6.94E-13
CFLAR-AS1	−1.032373666	−0.296510495	1.58E-13	7.68E-13
HOXA11-AS	4.166628873	−2.383791561	1.80E-13	8.67E-13
LINC01257	−2.181395918	−1.691533497	1.84E-13	8.86E-13
ZBTB20-AS4	−1.047497562	−2.989131549	1.92E-13	9.24E-13
LINC02185	−1.023094413	−2.891139184	1.95E-13	9.38E-13
LINC01968	1.48094991	−2.103467349	1.96E-13	9.42E-13
LINC00941	1.625347914	−1.387437985	3.78E-13	1.78E-12
LINC002481	1.495418772	−0.143266933	4.34E-13	2.03E-12
LINC02188	3.229751041	−1.527972609	5.12E-13	2.38E-12
SMIM2-AS1	1.178404954	0.322823782	5.69E-13	2.64E-12
LINC01356	1.190556663	−1.831840222	6.24E-13	2.88E-12
LINC02147	−1.072111191	−2.870655795	7.62E-13	3.48E-12
LINC01978	1.951430208	−2.980361568	8.71E-13	3.96E-12
LINC02159	2.397099936	−0.933800073	1.14E-12	5.13E-12
LINC01268	1.090115087	−1.303777324	1.17E-12	5.27E-12
BCRP3	1.172140497	1.694335748	1.23E-12	5.51E-12
CLDN10-AS1	4.005598887	−2.973381464	1.25E-12	5.62E-12
FENDRR	−1.087861902	−1.511265566	1.71E-12	7.58E-12
LINC00365	2.180566649	−2.173046848	1.77E-12	7.85E-12
VLDLR-AS1	−1.191609201	0.617764708	1.94E-12	8.57E-12
LINC01013	−1.467488426	−2.921867766	2.09E-12	9.21E-12
CHRM3-AS2	−1.729962854	−1.377369429	2.75E-12	1.20E-11
LINC02332	2.499668454	−2.643618803	2.87E-12	1.25E-11
EGOT	1.549008427	−0.516329627	3.23E-12	1.40E-11
LINC01122	1.495796901	−1.225533861	3.50E-12	1.51E-11
WARS2-IT1	−1.140761467	−2.892426107	3.84E-12	1.65E-11
MGAT3-AS1	1.921471241	−3.132315434	5.97E-12	2.52E-11
TMEM51-AS1	1.049425344	−0.278657046	6.93E-12	2.91E-11
DIO3OS	−1.732138449	−0.935519124	7.98E-12	3.34E-11
HHIP-AS1	−1.177273839	−1.574746134	8.47E-12	3.53E-11
PROX1-AS1	−1.492599784	0.164582035	9.37E-12	3.89E-11
MIR222HG	1.347824069	4.113966365	1.10E-11	4.52E-11
MKX-AS1	3.44096215	−2.962878331	1.12E-11	4.60E-11
TEX26-AS1	1.870701445	−1.304539618	1.91E-11	7.74E-11
C10orf91	1.347442868	−1.341693988	2.13E-11	8.58E-11
LINC01586	−1.487926787	0.577229992	2.53E-11	1.01E-10

LncRNA	logFC	logCPM	PValue	FDR
SRGAP3-AS4	−1.09460423	−3.018458492	6.20E-11	2.40E-10
LINC01215	−1.426380567	−0.611543209	7.13E-11	2.75E-10
MEG9	2.480937047	−2.417027462	7.48E-11	2.88E-10
LINC02516	1.681241882	−2.609607668	8.63E-11	3.30E-10
LINC01933	2.440700071	−0.575450993	1.08E-10	4.09E-10
LINC01451	1.738266137	−3.016532722	1.19E-10	4.49E-10
UCA1	3.111031028	−1.662934778	1.32E-10	4.94E-10
MIR646HG	1.587246721	0.823625444	1.38E-10	5.18E-10
PACERR	1.32108611	−1.739672921	1.71E-10	6.35E-10
PLAC4	−1.179131972	−3.187321626	1.73E-10	6.41E-10
LINC00402	−2.086388338	−2.423911662	1.79E-10	6.61E-10
LINC00113	1.878237395	−2.20315245	1.85E-10	6.83E-10
PRR29-AS1	1.288952449	−0.644369191	2.18E-10	7.99E-10
NAV2-AS5	−1.220830156	−3.044836102	2.38E-10	8.68E-10
LINC01781	−2.191172737	−2.280638527	2.99E-10	1.08E-09
LINC01366	1.180959368	−2.087149168	4.83E-10	1.71E-09
LY6E-DT	1.150565814	−0.744948928	4.93E-10	1.74E-09
LINC00877	−1.32562314	−1.54542177	5.02E-10	1.77E-09
TSIX	−1.082612999	−1.750693592	5.69E-10	2.00E-09
MLIP-IT1	−1.117952809	−2.859092371	6.15E-10	2.16E-09
LINC00861	−1.295589209	0.676313736	6.51E-10	2.28E-09
FALEC	2.187742734	−1.382164308	6.96E-10	2.43E-09
MYOSLID	1.742193737	−2.393689052	8.97E-10	3.10E-09
LINC00578	1.499995698	−1.310238231	1.10E-09	3.78E-09
TCL6	−1.947664766	−1.819781972	1.11E-09	3.80E-09
RNU6ATAC35P	−1.075599348	−2.207438516	1.15E-09	3.94E-09
FGF13-AS1	−1.228854208	−1.515972615	1.15E-09	3.95E-09
TMC3-AS1	−1.011789762	−1.059725645	1.46E-09	4.93E-09
LINC01705	3.308082231	−2.821752802	1.66E-09	5.56E-09
LINC01502	−2.098195941	−1.469981803	1.85E-09	6.17E-09
LINC00242	1.284297799	−0.439727608	1.91E-09	6.35E-09
LINC01857	−1.517930886	−1.450805986	2.34E-09	7.73E-09
LINC02080	1.136512753	−2.714119806	3.34E-09	1.09E-08
LINC02347	2.51584231	−3.178109564	3.42E-09	1.11E-08
LINC02384	−1.161842833	−1.106399342	4.33E-09	1.39E-08
LINC00892	−1.30588597	−1.896209333	6.93E-09	2.18E-08
IL12A-AS1	1.56757292	−2.176150296	7.87E-09	2.46E-08
RNF157-AS1	−1.079508605	1.476715592	9.97E-09	3.09E-08
LINC01843	1.297404227	−3.040632431	1.00E-08	3.10E-08
C8orf34-AS1	1.431387442	−2.031569466	1.34E-08	4.08E-08
LINC00574	1.305100436	−1.794608236	1.62E-08	4.92E-08
MIR205HG	2.350653908	0.546488105	1.73E-08	5.21E-08
PGM5P3-AS1	−1.066806842	−3.198234181	2.35E-08	6.99E-08
SMIM25	1.142177704	1.469520261	2.58E-08	7.65E-08

LncRNA	logFC	logCPM	PValue	FDR
MIR4527HG	2.188066145	−2.951448562	2.85E-08	8.39E-08
LINC01929	1.272249698	−2.125871713	3.08E-08	9.05E-08
DPP10-AS1	2.176483838	−1.655100877	3.13E-08	9.20E-08
LINC01293	2.967538508	−1.723191923	3.21E-08	9.42E-08
LINC02154	2.195301434	−2.804635425	3.76E-08	1.09E-07
KCCAT333	1.89311652	−2.130586927	4.04E-08	1.17E-07
LINC01934	−1.301524233	−2.654274876	4.18E-08	1.21E-07
LINC01133	−1.486025422	−2.743801026	4.34E-08	1.26E-07
LINC01480	−1.134594996	−0.252379128	4.91E-08	1.41E-07
LINC00836	3.169311285	−3.126967444	5.69E-08	1.63E-07
HPN-AS1	1.197442278	−1.9946336	5.94E-08	1.69E-07
LINC00958	1.16539197	2.956503057	6.23E-08	1.77E-07
EWSAT1	1.122167767	−2.725198589	7.62E-08	2.15E-07
C1QTNF1-AS1	1.078410505	−3.0366887	7.78E-08	2.19E-07
LINC01115	−1.318688616	−2.738546987	1.08E-07	2.99E-07
LINC00494	−1.671536378	−2.327283888	1.10E-07	3.05E-07
LINC00707	2.297861456	−2.959620206	1.13E-07	3.11E-07
LAMP5-AS1	3.188247546	−1.742057955	1.27E-07	3.50E-07
PTPRD-AS1	−1.071184828	0.033608176	1.34E-07	3.68E-07
PROSER2-AS1	−1.095640461	1.260536771	2.01E-07	5.41E-07
FLJ12825	1.23632278	−2.930254111	2.54E-07	6.74E-07
GLIS3-AS1	1.732029993	−0.478794145	3.40E-07	8.90E-07
IGF2-AS	3.625330184	−0.953350055	3.60E-07	9.41E-07
LINC00856	1.575984631	−2.870484623	3.79E-07	9.87E-07
RNF144A-AS1	1.321527479	−2.273405334	6.63E-07	1.69E-06
B3GALT5-AS1	−1.201277327	0.168991877	7.45E-07	1.89E-06
LINC00944	−1.071571769	−2.944872506	8.27E-07	2.08E-06
LINC02422	−1.541154888	−2.883560113	1.49E-06	3.64E-06
LINC01281	−1.430920089	−2.531665745	2.28E-06	5.45E-06
FAM83A-AS1	1.458937659	−2.114668914	2.77E-06	6.55E-06
LINC02273	−1.082325192	−1.828567427	3.17E-06	7.45E-06
LINC02542	1.070062828	−3.032499547	3.81E-06	8.87E-06
NKAIN3-IT1	2.571006542	−1.294499315	6.12E-06	1.39E-05
LINC01235	1.145275107	1.531217473	6.17E-06	1.40E-05
LINC02550	−1.012245336	−1.559729413	6.40E-06	1.46E-05
FAM30A	−1.532161339	1.318010816	6.50E-06	1.48E-05
SLC12A5-AS1	1.037143804	−2.421794006	6.89E-06	1.56E-05
LINC00940	−1.510161518	−1.854244335	9.61E-06	2.14E-05
LINC01885	−1.353714064	−1.056276139	1.13E-05	2.50E-05
LINP1	1.238363304	−2.399627643	1.32E-05	2.88E-05
CERS3-AS1	1.521145283	−3.208562221	1.78E-05	3.84E-05
LINC01010	1.224418357	−1.706364089	1.91E-05	4.11E-05
MIR3945HG	1.347395059	−2.382747989	2.19E-05	4.66E-05
LHX1-DT	3.941038665	−3.164857967	2.32E-05	4.94E-05

LncRNA	logFC	logCPM	PValue	FDR
LINC01976	−1.235919046	−2.611455982	2.95E-05	6.21E-05
LINC01597	1.180394892	−2.038545166	6.32E-05	0.000128067
DLX6-AS1	1.026349641	−1.509082087	7.11E-05	0.000142994
LINC00525	1.174432004	−2.731294734	8.64E-05	0.000172065
LINC02576	−1.187034556	−2.141212976	0.000102011	0.000201612
IFNG-AS1	−1.300736035	−1.972370504	0.000102388	0.000202312
SLC26A4-AS1	−1.007653022	8.554374474	0.000108694	0.000213992
LINC01783	1.058124593	−2.587925042	0.000118932	0.000232589
LINC01736	1.001949864	−2.238306481	0.000133039	0.000258681
LINC02544	1.125663027	−1.252983739	0.000205176	0.000389425
DGCR10	1.008940155	−2.906238751	0.000323916	0.000598487
LINC01016	2.014036935	−3.032889062	0.000527357	0.0009492
LINC02232	−1.397984509	−0.746262465	0.00080403	0.001413368
LINC00261	−1.065417538	−1.644636073	0.001219267	0.002090539
MIR1-1HG-AS1	1.541132604	−2.042776475	0.001329433	0.002268781
LINC01896	2.692433265	−2.185763054	0.00392824	0.006280554
LINC00648	1.296137264	−2.152158054	0.004459872	0.007064917
LINC01014	−1.014153989	−3.084912065	0.004587855	0.007252895
ZFY-AS1	−1.51394898	−0.614803454	0.004705264	0.007420158
LINC02506	1.825073446	−2.948330371	0.00535615	0.008366998

References:

1. Siegel RL, Miller KD, Jemal A: Cancer statistics, 2019. Cancer J Clin, 2019; 69: 7–34

2. Dralle H, Machens A, Basa J et al: Follicular cell-derived thyroid cancer. Nat Rev Dis Primers, 2015; 1: 15077

3. Davies L, Welch HG: Current thyroid cancer trends in the United States. JAMA Otolaryngol Head Neck Surg, 2014; 140: 317–22

4. Fagin JA, Wells SJ: Biologic and clinical perspectives on thyroid cancer. N Engl J Med, 2016; 375: 1054–67

5. Jung CK, Little MP, Lubin JH et al: The increase in thyroid cancer incidence during the last four decades is accompanied by a high frequency of BRAF mutations and a sharp increase in RAS mutations. J Clin Endocrinol Metab, 2014; 99: E276–85

6. Fagin JA, Mitsiades N: Molecular pathology of thyroid cancer: Diagnostic and clinical implications. Best Pract Res Clin Endocrinol Metab, 2008; 22: 955–69

7. Pak K, Suh S, Goh TS et al: BRAF-positive multifocal and unifocal papillary thyroid cancer show different messenger RNA expressions. Clin Endocrinol (Oxf), 2019; 90: 601–7

8. Landa I, Ibrahimpasic T, Boucai L et al: Genomic and transcriptomic hallmarks of poorly differentiated and anaplastic thyroid cancers. J Clin Invest, 2016; 126: 1052–66

9. Jendrzejewski J, Liyanarachchi S, Nagy R et al: Papillary thyroid carcinoma: Association between germline DNA variant markers and clinical parameters. Thyroid, 2016; 26: 1276–84

10. Zhang L, Peng D, Sood AK et al: Shedding light on the dark cancer genomes: Long noncoding RNAs as novel biomarkers and potential therapeutic targets for cancer. Mol Cancer Ther, 2018; 17: 1816–23

11. Ma L, Cao J, Liu, L et al: LncBook: A curated knowledgebase of human long non-coding RNAs. Nucleic Acids Res, 2019; 47: D128–34

12. Beltran M, Puig I, Pena C et al: A natural antisense transcript regulates Zeb2/Sip1 gene expression during Snail1-induced epithelial-mesenchymal transition. Genes Dev, 2008; 22: 756–69

13. Munroe SH, Lazar MA: Inhibition of c-erbA mRNA splicing by a naturally occurring antisense RNA. J Biol Chem, 1991; 266: 22083–86

14. Wang H, Iacoangeli A, Lin D et al: Dendritic BC1 RNA in translational control mechanisms. J Cell Biol, 2005; 171: 811–21

15. Braidotti G, Baubec T, Pauler F et al: The air noncoding RNA: An imprinted cis-silencing transcript. Cold Spring Harb Symp Quant Biol, 2004; 69: 55–66

16. Bhan A, Soleimani M, Mandal SS: Long noncoding RNA and cancer: A new paradigm. Cancer Res, 2017; 77: 3965–81

17. Peng WX, Koirala P, Mo YY: LncRNA-mediated regulation of cell signaling in cancer. Oncogene, 2017; 36: 5661–67

18. Ding H, Liu J, Zou R et al: Long non-coding RNA TPTEP1 inhibits hepatocellular carcinoma progression by suppressing STAT3 phosphorylation. J Exp Clin Cancer Res, 2019; 38: 189

19. Yu S, Yang D, Ye Y et al: LncRNA AFAP1-AS1 promotes malignant phenotype through binding with LSD1 and repressing HBP1 in non-small cell lung cancer. Cancer Sci, 2019; 110(7): 2211–25

20. Zhao Q, Sun J: Cox survival analysis of microarray gene expression data using correlation principal component regression. Stat Appl Genet Mol Biol, 2007; 6: e16

21. Li B, Zhao W, Xu L et al: Minimally invasive video-assisted lateral neck lymphadenectomy for the papillary thyroid carcinoma with cervical lymph nodes metastasis. J Clin Oncol, 2016; 46: 635–41

22. Qi L, He W: REGgamma is associated with lymph node metastasis and T-stage in papillary thyroid carcinoma. Med Sci Monit, 2018; 24: 1373–78

23. Li HM, Yang H, Wen DY et al: Overexpression of LncRNA HOTAIR is associated with poor prognosis in thyroid carcinoma: A study based on TCGA and GEO data. Horm Metab Res, 2017; 49: 388–99

24. Wang Y, He H, Li W et al: MYH9 binds to lncRNA gene PTCSC2 and regulates FOXE1 in the 9q22 thyroid cancer risk locus. Proc Natl Acad Sci USA, 2017; 114: 474–79

25. Zhu H, Lv Z, An C et al: Onco-lncRNA HOTAIR and its functional genetic variants in papillary thyroid carcinoma. Sci Rep, 2016; 6: 31969

26. Guo K, Chen L, Wang Y et al: Long noncoding RNA RP11-547D24.1 regulates proliferation and migration in papillary thyroid carcinoma: Identification and validation of a novel long noncoding RNA through integrated analysis of TCGA database. Cancer Med, 2019; 8(6): 3105–19

27. Fagerberg L, Hallstrom BM, Oksvold P et al: Analysis of the human tissue-specific expression by genome-wide integration of transcriptomics and antibody-based proteomics. Mol Cell Proteomics, 2014; 13: 397–406

28. Akamatsu S, Takata R, Haiman CA et al: Common variants at 11q12, 10q26 and 3p11.2 are associated with prostate cancer susceptibility in Japanese. Nat Genet, 2012; 44: 426–29, S1

29. Fernandez-Retana J, Zamudio-Meza H, Rodriguez-Morales M et al: Gene signature based on degradome-related genes can predict distal metastasis in cervical cancer patients. Tumour Biol, 2017; 39: 1393377769

30. Lee KY, Huang SM, Li S, Kim JM: Identification of differentially expressed genes in papillary thyroid cancers. Yonsei Med J, 2009; 50: 60–67

31. Gomez-Rueda H, Palacios-Corona R, Gutierrez-Hermosillo H, Trevino V: A robust biomarker of differential correlations improves the diagnosis of cytologically indeterminate thyroid cancers. Int J Mol Med, 2016; 37: 1355–62

32. Jarzab B, Wiench M, Fujarewicz K et al: Gene expression profile of papillary thyroid cancer: Sources of variability and diagnostic implications. Cancer Res, 2005; 65: 1587–97

33. Galeza-Kulik M, Zebracka J, Szpak-Ulczok S et al: [Expression of selected genes involved in transport of ions in papillary thyroid carcinoma]. Endokrynol Pol, 2006; 57(Suppl. A): 26–31 [in Polish]

34. Yerukala SS, Sahu D, Huang HC et al: Identification and characterization of the lncRNA signature associated with overall survival in patients with neuroblastoma. Sci Rep, 2019; 9: 5125

35. Plymate SR, Bhatt RS, Balk SP: Taxane resistance in prostate cancer mediated by AR-independent GATA2 regulation of IGF2. Cancer Cell, 2015; 27: 158–59